

## Subcooled two-phase flow boiling in a microchannel heat sink: comparison of conventional numerical models

Ali Soleimani<sup>a</sup>, Pedram Hanafizadeh<sup>a,\*</sup> and Amirmohammad Sattari<sup>a</sup>

<sup>a</sup> School of Mechanical Engineering, College of Engineering, University of Tehran, Iran

### ARTICLE INFO

#### Article history:

Received: 23 July 2019

Accepted: 2 December 2019

#### Keywords:

Subcooled flow boiling

Microchannel

Heat sink

CFD

VOF model

### ABSTRACT

Subcooled flow boiling in multi-microchannels can be used as an efficient thermal management approach in compact electrical devices. Highly subcooled flow boiling of HFE 7100 is studied in two microchannel heat sinks to choose a proper numerical model for simulating boiling flows in microchannels. Results of five different numerical models, including Volume of Fluid (VOF), Eulerian boiling, Eulerian Lee, Eulerian thermal phase change, and mixture models, were compared with experimental data. ANSYS Fluent was used as the numerical tool to solve three-dimensional governing equations. Results were obtained in the steady-state condition of the transient solution. The average wall temperature reached a steady state in all models except in Eulerian boiling and mixture models. It was found that Eulerian thermal phase change and VOF models predicted microchannel's bottom wall average temperature with less than 2% error. VOF model predicted flow boiling regime as it was reported in the experimental research and boiling curves. Velocity distribution over microchannel height was investigated, and it was observed that after the onset of nucleate boiling, the velocity profile becomes asymmetrical. Also, in the two-phase regions, each phase had a different velocity magnitude and distribution. Based on flow regime and temperature results, which were compared with experimental data, VOF model was recommended as the best model to simulate flow boiling in microchannels at the working conditions of this research. Furthermore, subcooled flow boiling's capability to be used in thermal management systems was proved while observing temperature distribution over computational domain.

### 1. Introduction

With recent developments in high power electronic devices, their power consumption is growing as well. So, these new electronic devices dissipate higher heat than the older ones. This dissipated heat needs to be removed from the devices to ensure their proper working conditions. Besides, there is a trend toward making dimensions of electronic devices smaller. In this situation, a small device dissipates a large amount of heat, which is called a high heat flux device. With this dissipated heat, device temperature rises. The condition of high temperature can interrupt the performance of the electronic device or cause serious damage to the device. Hereby, conventional methods should be modified to meet the needed thermal performance of the device. In 1981, Tuckerman et al. [1] offered to employ microchannels for cooling of high heat flux devices. The device they used in their research is well-known as microchannel heat sink (MCHS).

Microchannel is referred to a channel or tube which its characteristic length is below 1 mm. In a study, Ong and Thome [2] researched macro to micro behaviors in two-phase flows, and they suggested a new scale for macro to microscale transition

criterion. This new scale criterion was higher than the scales used in previous studies. Based on the square-cube law [3] as the size of a channel gets smaller, its surface to volume ratio increases significantly. Because of heat transfer proportionality to the surface, it is expected that in microchannels heat transfer performance grows notably. Hatami and Ganji [4] investigated thermal performance of microchannel heat sinks. They concluded that microchannels with smaller channel width have a higher Nusselt number. Salman et al. [5] also reported microchannels with smaller size have higher heat transfer coefficient.

It is well known that electronic devices have a maximum working temperature limit. So, thermal management approaches should face this fact and be able to minimize the temperature of the device. The fact that the temperature of the fluid is fixed to the saturated temperature of the fluid is the key feature of the boiling phenomenon. Thus, using flow boiling in microchannels can be a very efficient method in microelectronics cooling. Morshed et al. [6] studied flow boiling in microchannels and reported an increase in the heat transfer coefficient by using two-phase flow boiling. Harirchian and Grimella [7] also investigated flow boiling in microchannels as a cooling solution for high heat flux devices.

\* Corresponding author. Tel.: +98 61119999; Fax: +98 61119999; e-mail: [hanafizadeh@ut.ac.ir](mailto:hanafizadeh@ut.ac.ir)

They developed a flow regime map that included bubbly, annular, slug, and churn flow patterns. Agostini et al. [8] studied refrigerant boiling in multi-microchannels. They examined effect of vapor quality on heat transfer coefficient and identified three different characteristic tendencies for heat transfer coefficient. Lee and Pan [9] studied geometrical effects on boiling heat transfer in a single microchannel. They concluded that a diverging cross-section makes two-phase flow fluctuations more stable and has a better heat transfer performance. In another research, a sub-ambient subcooled flow boiling in a microchannel heat sink was investigated by Lee and Mudawar [10] experimentally. They observed flow boiling regimes at different heat fluxes and concluded that subzero inlet temperatures are capable of dissipating heat fluxes as high as 700 W/cm<sup>2</sup>. Temperature distribution in a fin was studied in different boiling conditions by Oguntalaa et al. [11], and it was concluded that temperature dispersion along the fin length decreases for higher boiling condition parameters.

Studying the boiling phenomenon numerically is a matter of computational effort. Choosing a suitable multiphase algorithm is the first and most important step. Here, a short review of conventional multiphase models used in macroscale boiling simulations is presented. Alizadehdakhel et al. [12] studied flow and heat transfer of a thermosiphon numerically. They used a two-dimensional domain and employed the VOF (volume of fluid) model to capture two-phase evaporation. The VOF model was also applied in flow boiling inside a macroscale pipe by Kuang et al. [13]. They observed flow characteristics and patterns in their three-dimensional domain. In another research, Abedini et al. [14] used the mixture model formulation to solve subcooled boiling flow. They did not report any observation on the two-phase flow regimes. Recently, Behroyan et al. [15] studied Eulerian based models in subcooled flow boiling. They used a two-dimensional domain for their macroscale pipe.

Flow boiling in microscale is also in the scope of numerical studies' interest. Mukherjee and Kandlikar [16] simulated the growth of a single bubble in a microchannel by using the level-set method. They showed that bubble movement can enhance heat transfer and the influence of gravity on bubble growth is small. The level-set model was also used in another study by Mukherjee et al. [17]. They investigated effect of surface tension on Besidessingle bubble growth in a microchannel. They concluded that effect of surface tension on heat transfer is negligible, but its effect on bubble shape is significant. Magnini et al. [18] studied flow and heat transfer of single bubble growth in a microchannel. They employed a VOF based model to capture volume fraction of each phase. In another study, Fang et al. [19] investigated flow boiling in a microchannel using VOF model. Zhuan and Wang [20] studied flow boiling of refrigerants in a microtube numerically. They used VOF model and observed flow patterns of flow boiling. It was reported that with lower saturated temperature, liquid surface tension is higher and bubbles coalesce easier. Zhuan and Wang [21] researched subcooled flow boiling using the numerical tool. They employed VOF model formulation and verified their numerical model by comparing flow patterns with some experimental results. They concluded that in channels with high aspect ratio cross-sections the Onset of Nucleate Boiling (ONB) occurs at a higher distance from the inlet.

As mentioned, selecting the appropriate model is vital for numerical simulation of two-phase flows, especially those contain boiling phenomena. However, to the author's knowledge, there is a lack of works that investigated various models in a comprehensive study. With the aim of filling this gap, subcooled

flow boiling in two microchannels is simulated using five different models. The flow boiling regime at working conditions is presented and compared with the boiling curves of the working fluid. The average bottom wall temperature at steady state is reported for all models, and it is compared with experimental data. Based on preciseness of wall temperature and boiling flow pattern prediction a suitable model among used models is introduced. Some thermal and flow specifications of the selected model are investigated in order to have a better view of boiling phenomenon in microchannels.

## 2. Methodology

### 2.1. Governing equations

To solve the equations related to both phases in boiling, three conventional multiphase models, including volume of fluid (VOF), mixture, and Eulerian, were employed. In these models, all phases are considered incompressible, and fluid flow is assumed to be Newtonian. Here, the main equations of these models are presented. Afterward, the mass transfer mechanisms used in this research are explained.

#### 2.1.1. VOF model

Solving a single set of momentum and energy equations is the feature of the VOF model. In addition, this model solves an equation to monitor changes in the volume fraction of each phase. The VOF model cannot be used for miscible phases, and every cell in the computational domain must conclude at least one of the phases. The case that two phases coexist in a cell represents the interface between those phases. Volume fraction equation which is based on the continuity for  $q^{th}$  phase is as follows [22]:

$$\frac{1}{\rho_q} \left[ \frac{\partial}{\partial t} (\alpha_q \rho_q) + \nabla \cdot (\alpha_q \rho_q \vec{v}_q) \right] = \sum_{p=1}^n (\dot{m}_{pq} - \dot{m}_{qp}) \quad (1)$$

where  $\dot{m}_{pq}$  is the mass transfer from phase  $p$  to phase  $q$ ,  $\dot{m}_{qp}$  is the mass transfer from phase  $q$  to phase  $p$  and  $\alpha_q$  is the volume fraction of  $q^{th}$  phase. The volume fraction of primary phase is calculated based on the fact that at each cell, sum of volume fraction of all phases is unity:

$$\sum_{q=1}^n \alpha_q = 1 \quad (2)$$

#### 2.1.2. Eulerian model

In the Eulerian-Eulerian formulation, all conservation laws are solved for each phase separately. Therefore, this multiphase model has a high computational cost. The continuity equation is the same as the volume fraction equation of the VOF model which is presented in Eq. 1. The momentum equation that is solved for  $q^{th}$  phase in this model is as follows [22]:

$$\begin{aligned} \frac{\partial}{\partial t} (\alpha_q \rho_q \vec{v}_q) + \nabla \cdot (\alpha_q \rho_q \vec{v}_q \vec{v}_q) \\ = -\alpha_q \nabla p + \nabla \cdot \bar{\tau}_q + \alpha_q \rho_q \vec{g} \\ + \sum_{p=1}^n (\vec{R}_{pq} + \dot{m}_{pq} \vec{v}_{pq} - \dot{m}_{qp} \vec{v}_{qp}) \\ + (\vec{F}_q + \vec{F}_{vm,q}) \end{aligned} \quad (3)$$

where  $\vec{F}_q$  and  $\vec{F}_{vm,q}$  are external body force and virtual mass force, respectively. The term  $\bar{\tau}_q$  is a variable that is related to the stress-strain. The terms  $\vec{v}_{pq}$  and  $\vec{v}_{qp}$  are interphase velocity and the interphase force, which is expressed by  $\vec{R}_{pq}$ . The energy is preserved by solving the energy equation, which can be formulated for the  $q^{th}$  phase as [22],

$$\begin{aligned} \frac{\partial}{\partial t}(\alpha_q \rho_q h_q) + \nabla \cdot (\alpha_q \rho_q \vec{u}_q h_q) \\ = \alpha_q \frac{d p_q}{d t} + \bar{\tau}_q \cdot \nabla \vec{u}_q - \nabla \cdot \vec{q}_q + S_q \\ + \sum_{p=1}^n (Q_{pq} + \dot{m}_{pq} h_{pq} - \dot{m}_{qp} h_{qp}) \end{aligned} \quad (4)$$

where  $h_q$ ,  $\vec{q}_q$  and  $S_q$  are specific enthalpy, heat flux, and enthalpy source term, respectively. In this equation,  $Q_{pq}$  represents the intensity of heat exchange.

### 2.1.3. Mixture model

The mixture model is a multiphase model with reduced complexity. This model assumes that the actual multiphase flow is a single-phase flow with corrected properties for each phase. The continuity equation for this model is represented as,

$$\frac{\partial}{\partial t}(\rho_m) + \nabla \cdot (\rho_m \vec{v}_m) = 0 \quad (5)$$

where a mass averaged formulation is used to calculate  $\vec{v}_m$ . The term  $\rho_m$  is the mixture density and is derived using volume fraction ( $\alpha_q$ ) based formulation:

$$\rho_m = \sum_{q=1}^n (\alpha_q \rho_q) \quad (6)$$

The momentum equation can be derived by summing momentum equation of every phase, and its formulation is presented as

$$\begin{aligned} \frac{\partial}{\partial t}(\rho \vec{v}) + \nabla \cdot (\rho \vec{v} \vec{v}) \\ = -\nabla p + \nabla \cdot [\mu(\nabla \vec{v} + \nabla \vec{v}^T)] + \rho \vec{g} \\ + \vec{F} - \nabla \cdot \left( \sum_{q=1}^n \alpha_q \rho_q \vec{v}_{dr,q} \vec{v}_{dr,q} \right) \end{aligned} \quad (7)$$

here  $\vec{v}_{dr,q}$  is the drift velocity of  $q^{th}$  phase. The energy equation for the  $q^{th}$  phase of  $n$  phases is as follows [22]:

$$\begin{aligned} \frac{\partial}{\partial t} \sum_{q=1}^n (\alpha_q \rho_q E_q) + \nabla \cdot \sum_{q=1}^n (\alpha_q \vec{v}_q (\rho_q E_q + p)) \\ = \nabla \cdot (k_{eff} \nabla T) + S_h \end{aligned} \quad (8)$$

The properties of all variables are the same as described variables in former models.

### 2.1.4. Mass transfer mechanisms

Boiling phenomena is a mass transfer from the liquid phase to the vapor phase. Mass transfer mechanisms are used by employing models that were developed based on experimental correlations. In this research, three well-known formulations are used to simulate flow boiling in microchannels. These formulations include Lee's

model, boiling model, and thermal phase change model [22]. The Lee model formulation is employed to VOF, Eulerian and mixture multiphase models. The boiling model and the thermal phase-change formulations are only used in the Eulerian multiphase model.

The mass transfer mechanism used to model flow boiling in the Lee model is based on Lee's two-phase modeling scheme [23]. In this model, criteria for occurring mass transfer from liquid phase ( $l$ ) to the vapor phase ( $v$ ) is the temperature of liquid phase. Hence, if liquid temperature ( $T_l$ ) is higher than the saturation temperature ( $T_{sat}$ ), this mass transfer ( $\dot{m}_{lv}$ ) is calculated as,

$$\dot{m}_{lv} = C \cdot \alpha_l \rho_l \frac{(T_l - T_{sat})}{T_{sat}} \quad (9)$$

where  $C$  is a constant coefficient that can be calculated from the physical properties of the working fluids.

The boiling model is based on the fact that a part of the energy, which is transferred from the wall to the liquid, causes liquid temperature increase and the other part causes a phase change. This model was first developed in the Rensselaer Polytechnic Institute (RPI) by Kurul [24]. The part of wall heat flux that causes phase change ( $\dot{q}_E$ ) has a relation with bubble departure diameter ( $D_w$ ):

$$\dot{q}_E \propto D_w^{-\frac{1}{2}} \quad (10)$$

So, by calculating the bubble departure diameter, the heat flux of evaporation and, consequently, the mass transfer from the liquid phase to the vapor phase can be derived. The bubble diameter (in meters) is calculated using an experimental correlation of Tolubinsky and Kostanchuk [25],

$$D_w = \min(0.0014, 0.0006e^{-\Delta T_{sub}/45}) \quad (11)$$

where the term  $\Delta T_{sub}$  is the degree of subcooling. The bubble departure diameter calculated from this equation is in order of microchannel height. Hence, it is expected that the formed bubble occupies the entire channel cross-section in form of a confined bubble. It is essential to consider those empirical correlations that are not developed in microscale channels, and researches are obliged to use these available data. In the boiling model formulation, the mass transfer from liquid phase to the vapor phase ( $\dot{m}_{lv}$ ) is calculated from

$$\dot{m}_{lv} = \frac{\dot{q}_E}{h_{lv} + C_{p,l} \Delta T_{sat}} \quad (12)$$

The thermal phase change model calculates mass transfer at the interface based on a heat balance between two phases. This formulation considers the heat transfer of each phase surface separately. Therefore, mass transfer of evaporation ( $\dot{m}_{lv}$ ) is calculated as follows:

**Table 1.** A brief description of the models used in this research and their appellation.

Multiphase model	Mass transfer equation	Appellation
VOF	Lee model (eq. 9)	<b>VOF Model</b>
Eulerian	Boiling model (eq. 12)	<b>EulBoil Model</b>
Eulerian	Lee model (eq. 9)	<b>EulLee Model</b>
Eulerian	Thermal phase change model (eq. 13)	<b>EulTPC Model</b>
Lee model (eq. 9)		<b>Mixture Model</b>

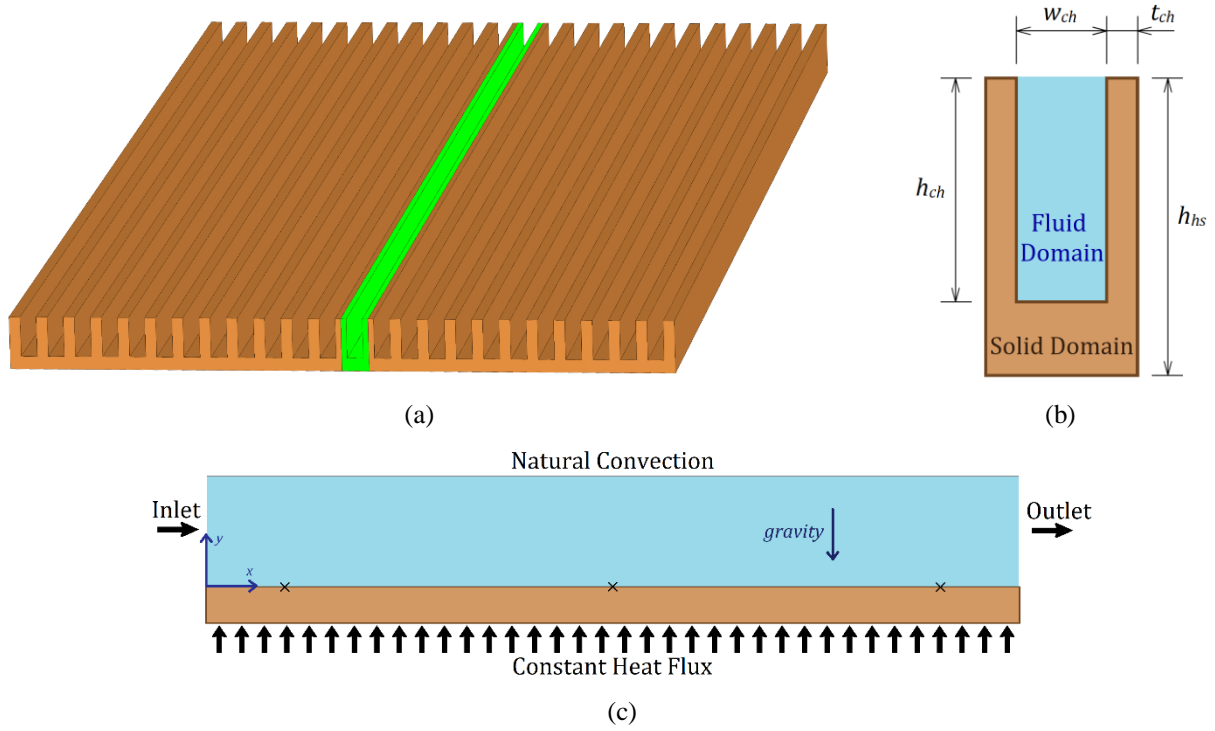


**Figure 1.** a) Schematic of the copper microchannel heat sink of HS#1. The computational domain is highlighted. b) Two-dimensional picture of one channel crosssection. c) mid-plane of the microchannel and main boundary conditions.

**Table 2.** geometrical dimensions and physical boundary conditions of the computational domain.

Case	$h_{ch}$ ( $\mu\text{m}$ )	$w_{ch}$ ( $\mu\text{m}$ )	$t_{ch}$ ( $\mu\text{m}$ )	$h_{hs}$ ( $\mu\text{m}$ )	$G$ ( $\text{kg}/\text{m}^2 \text{ s}$ )	$q''$ ( $\text{W}/\text{cm}^2$ )	$T_{in}$ ( $^{\circ}\text{C}$ )
HS#1	304.9	123.4	42.1	404.9	2215	173.3	-30

$$\dot{m}_{lv} = - \frac{h_l A_i (T_{sat} - T_l) + h_v A_i (T_{sat} - T_v)}{H_{vs} - H_{ls}} \quad (13)$$

where the terms  $h_l$  and  $h_v$  are heat transfer coefficients of liquid and vapor phases, respectively. The liquid and vapor enthalpies are expressed by  $H_{ls}$  and  $H_{vs}$ . A brief description of five numerical models is illustrated in Table 1. These models are used to simulate flow boiling in a microchannel, and henceforth they are going to be referred with the names listed in this table.

### 2.2. Computational domain and boundary conditions

In this research, a microchannel heat sink geometry from the experimental research of Lee and Mudawar [10] is investigated, which was utilized for observation of flow boiling in microchannel heat sinks. The schematic of the microchannel heat sink used in this study is shown in Fig. 1. The heat sink has 24 channels, and to simplify calculations, only one channel of heat sink, which is highlighted in Fig. 1a, will be used as the computational domain. This microchannel is labeled as ‘HS#1’. As it is shown in Fig. 1b, the computational domain consists of a solid domain and a fluid domain. Side view of the microchannel and main boundary conditions is displayed in Fig. 1c. The microchannel length is not to scale in this figure. The solid domain material is copper with thermal conductivity of 387.6 W/m K. The fluid used in this research is HFE 7100, and its thermophysical properties are employed using reported values of Lee and Mudawar [10]. The saturation temperature of HFE 7100 is 60 °C at atmospheric pressure. Dimensions of computational domain along with

physical boundary conditions are tabulated in Table 2. The channel length in this geometry is 10 mm.

In the experimental setup, it was reported that the top surface of the microchannels is closed using a 2 mm transparent lexan plate. So, in the numerical model, natural convection to ambient temperature and one-dimensional heat conduction in the lexan plate boundary conditions are employed on the top surfaces of solid and fluid domains. The fluid enters from one channel end and leaves the domain from the other one. Based on the experimental data [10] and as it is listed in Table 2, at all working conditions constant inlet temperature of -30 °C and inlet mass flux of 2215 kg/m<sup>2</sup>s is used. Also, a uniform heat flux of 173.3 W/cm<sup>2</sup> is applied to the heat sink base. The symmetry boundary condition is used at cut surfaces of solid domain. All of the fluid flows of this research are considered as continuum flows, and therefore, a no-slip boundary condition is used in the interfaces of solid and fluid domains. The temperature value in three equidistant points at the bottom of the channel will be probed, and the average of these values will be used as the average bottom wall temperature ( $\bar{T}_w$ ). These three points are 1.2, 5.0, and 8.8 mm away from the channel inlet, respectively and they are illustrated in Fig. 1c using black cross marks.

### 2.3. Numerical procedure

The commercial ANSYS Fluent V18.2 software was utilized as the numerical tool. This software solves governing equations by discretizing them based on the Finite Volume Method (FVM). The nature of boiling phenomena is transient, and its numerical

simulation cannot be done with steady formulation. Hence, numerical time-stepping is constrained with a fixed courant number (*CFL*) of 0.9. In ANSYS Fluent software, each time step ( $\Delta t$ ) is calculated using the following equation [22]:

$$\Delta t = \frac{CFL}{\max(\sum FPV)} \quad (14)$$

where the term *FPV* is outgoing fluxes per volume of each cell. In Eulerian and VOF multiphase models, this method of variable time stepping is used and, in the mixture multiphase model, a fixed time-stepping method is employed. For pressure-velocity coupling, the Pressure-Implicit with Splitting of Operators (PISO) algorithm is applied in VOF model and the Semi-Implicit Method for Pressure Linked Equation (SIMPLE) algorithm is applied in Eulerian and mixture models. Initial temperature distribution on both fluid and solid domains is considered uniform with the value of inlet temperature. In addition, the fluid is considered to be immobile at the initial state. All solutions are calculated until steadiness of average wall temperature ( $\bar{T}_w$ ) was reached. To obtain the time step in which the solution has reached steady state, percent of deviation of wall temperature value of that time step from root mean square of wall temperature at ten consecutive previous time steps was calculated. Thereafter, if for two successive time steps this value was less than 1%, that time step is considered to be end of the unsteady region of time. This steadiness criterion is applied to all models (except the ones that do not reach steadiness) to calculate wall temperature at steady conditions.

#### 2.4. Mesh independency

The three-dimensional geometries of computational domains have meshed with hexahedral cells. To capture gradients accurately, finer mesh is constructed for fluid domain near the walls. In order to reduce numerical errors, the effect of mesh density on numerical results is studied for HS#1 using the VOF multiphase model as the base model. The volume fraction of phases cannot be independent of mesh density, and for denser meshes smaller bubbles in size of smallest cells appear in the fluid domain. This dependency of volume fraction on mesh density affects other results of variables including temperature field. Therefore, in mesh study of a multiphase flow it is expected to minimize errors caused by different cell sizes but not to remove these errors.

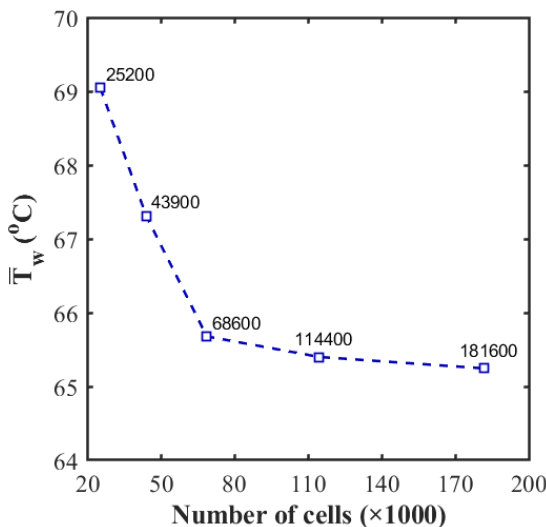


Figure 2. Average wall temperature ( $\bar{T}_w$ ) for different number of cells for HS#1. The results correspond to the VOF model.

As it is shown in Fig. 2, the average wall temperature ( $\bar{T}_w$ ) is plotted for different numbers of cells. Changes in  $\bar{T}_w$  has become slighter for higher number of cells than 68600. Hence, the mesh with 68600 cells will be used for numerical computations of this research.

### 3. Results and discussion

Flow boiling in computational domains is simulated using the presented formulations and numerical models. Volume fraction distributions of all models near the microchannel outlet of HS#1 are displayed in Fig. 3. In this case, the inlet flow temperature of the highly subcooled fluid is -30 °C. At the heat flux of 173.3 W/cm<sup>2</sup> and mass flux of 2215 kg/m<sup>2</sup>s, boiling starts at approximately 55 ms. Therefore, these contours are derived at three different times of 90 ms, 120 ms, and 150 ms, and they are plotted on the mid-plane of the channel, which is perpendicular to the channel bottom surface. As it is displayed in this figure, all models except VOF model and EulBoil model, have film boiling regime in which a film of vapor is formed on the wall surface. In the EulLee model, the vapor film is thicker than vapor film in other models including mixture model and EulTPC model. Therefore, it is concluded that EulLee formulation has a higher mass transfer from liquid to vapor phase than other models. In the VOF model, nucleate boiling regime can be noticed.

In the EulBoil model, a thin layer of HFE 7100 vapor is observed on the microchannel bottom surface at 90 ms and 120 ms. Within 130 ms, a bubble is formed, which takes almost the whole microchannel length. As it was expected from bubble diameter correlation (Eq. 11), the formed bubble occupies the entire microchannel cross-section in the EulBoil model. In this model, time-stepping is constrained with fixed courant number. This bubble increases the *FPV* term in courant number equation (Eq. 14) significantly, and as a result the time step size decreases to values in order of 1e-15 s. With this time step size and its trend to decrease, a very high computational cost is imposed and it was decided to use derived data up to 130 ms as the numerical results for EulBoil model.

Changes in average wall temperature ( $\bar{T}_w$ ) with time for all five models is displayed in Fig. 4. Solid lines are the numerical models, and the dashed line is the reported value of average wall temperature by Lee and Mudawar [10]. Three models including EulLee, EulTPC, and VOF models seem to have good agreement with experimental data. Using the steadiness criterion, it was observed that these three models reached a steady-state condition after approximately 130 ms. The mixture model did not reach the steady-state condition as its wall temperature increased monotonically. It shows that the mixture model formulation cannot predict wall temperature in flow boiling. Formulation of Eulerian based models and VOF model have a control on vapor temperature to not increase unreasonably. Also, the EulBoil model did not reach steady-state and its calculations were stopped while its average wall temperature value was 52 °C above the reported experimental value.

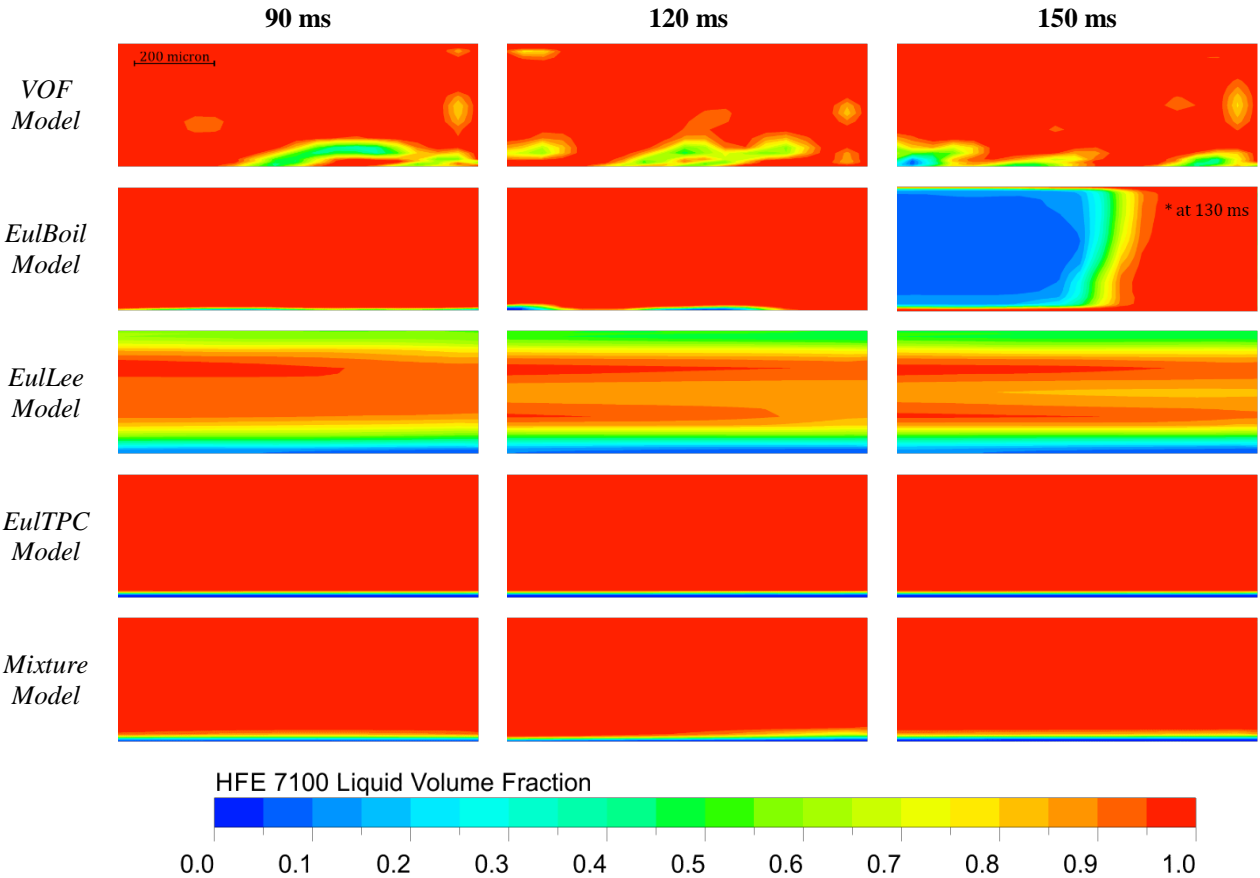


Figure 3. volume fraction distribution of all models near the microchannel exit/outlet of HS#1 at 90 ms, 120 ms and 150 ms for  $G=2215 \text{ kg/m}^2\text{s}$  and  $q''= 173.3 \text{ W/cm}^2$ .

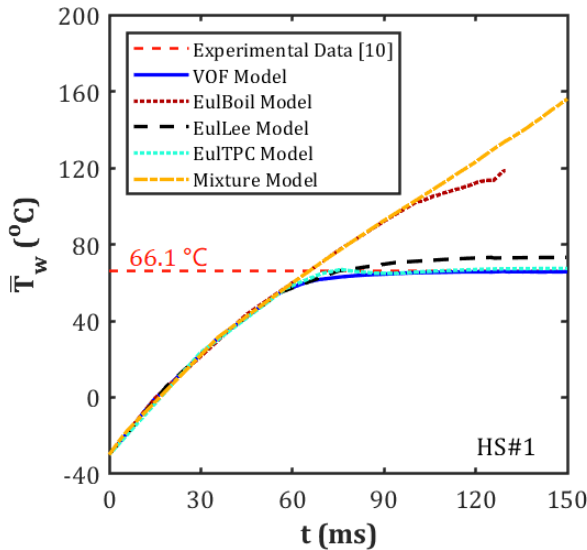


Figure 4. average wall temperature ( $\bar{T}_w$ ) with time for all five models for HS#1 at  $G=2215 \text{ kg/m}^2\text{s}$  and  $q''= 173.3 \text{ W/cm}^2$ .

The exact value of the average wall temperature ( $\bar{T}_w$ ) derived from all five models is listed in Table 3. This value is reported at steady state condition for all models except the mixture model and EulBoil model which did not reach steady state. The VOF model and the EulTPC model predicted  $\bar{T}_w$  with less than 2% error. In addition, the wall temperature was calculated with 10.6% of error

by the EulLee model. Hence, three models including VOF model, EulTPC model, and EulLee model have the potential to be selected as the suitable model to simulate flow boiling in a microchannel. Also,  $\bar{T}_w$  value derived using the EulBoil model is reported at 130 ms. It was concluded that this model cannot predict wall temperature value precisely.

Table 3. average wall temperature ( $\bar{T}_w$ ) for all models at steady-state and error percent with respect to experimental data for HS#1 at  $G=2215 \text{ kg/m}^2\text{s}$  and  $q''=173.3 \text{ W/cm}^2$ .

	$\bar{T}_w$ (°C)	Error (%)
<i>Experimental Data [10]</i>	66.1	-
<i>VOF Model</i>	65.7	0.61
<i>EulBoil Model</i>	118 <sup>†</sup>	78.5
<i>EulLee Model</i>	73.1	10.6
<i>EulTPC Model</i>	67.3	1.82
<i>Mixture Model</i>	156 <sup>††</sup>	136

The saturation temperature of HFE 7100 is 60 °C. Wall superheat, which is the difference between wall temperature and the saturation temperature, is found to be 9 °C at the region near the microchannel exit. Misale et al. [26] and also Lee and Mudawar [10] reported the boiling curve for HFE 7100 fluid.

Based on these researches, boiling flows with wall superheat bellow 11 °C can be considered nucleate boiling. Consequently, boiling regime for HS#1 is expected to be nucleate boiling. As it is shown in Fig. 3, only VOF model predicted this two-phase flow regime precisely. Despite proper wall temperature predicted by EulLee model and EulTPC model, they did not simulate boiling regime correctly, and therefore, they cannot be selected as a proper model for flow boiling in a microchannel. Hereby, the VOF model is introduced as the best model to simulate flow boiling and predict wall temperature with high precision.

To better investigate the VOF model, a set of results at 139.6 ms, including volume fraction, temperature and vectors distribution is displayed in Fig. 5. These results are plotted on the mid-plane of the HS#1 microchannel near its outlet. At this time step, a detaching bubble from microchannel bottom surface can be recognized. In the vectors' distribution, bigger vectors correspond to higher velocity magnitude. The core of the detaching bubble has a higher velocity magnitude than surrounding fluids. Hence, it has accelerated to leave microchannel base with liquid flow. In the temperature distribution (Fig. 5b), bubble core's interface is displayed with black lines. It is observed that bubble's heat has dissipated to surrounding liquid and it has caused a higher temperature distribution around the bubble. As a result of this, core temperature of the almost detached bubble is decreased to lower than saturation temperature. Therefore, it is most probable that this bubble shrinks in the process of condensation.

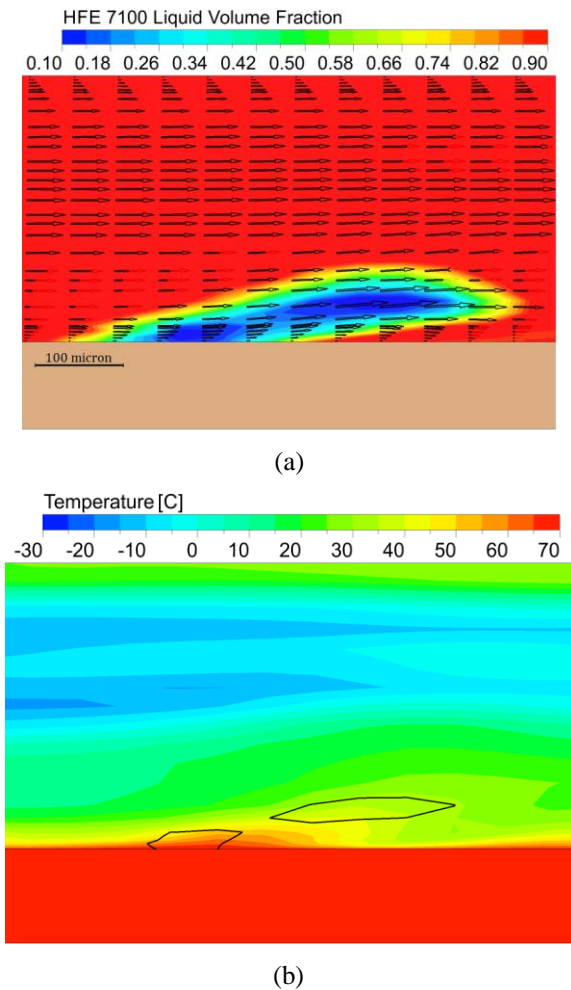


Figure 5. a) volume fraction and vector b) temperature distribution of the VOF model over HS#1 mid-plane at 139.6 ms for  $G=2215 \text{ kg/m}^2\text{s}$  and  $q''=173.3 \text{ W/cm}^2$ .

In addition, Fig. 5 confirms the fact that subcooled flow boiling in a set of microchannels is an effective method for thermal management. In this case, with a heat flux as high as  $173.3 \text{ W/cm}^2$  microchannel's base maximum temperature is below  $70 \text{ }^\circ\text{C}$ . In flow boiling phenomenon, this maximum temperature can be controlled by the saturation temperature of the working fluid.

As it was observed, the vapor core of detaching bubble had a higher velocity than its surrounding liquid. To better investigate this velocity difference, longitudinal velocity distribution at the location of the detaching bubble, which is  $x/L = 0.96$ , is plotted besides velocity distribution at two other locations, including  $x/L = 0.3$  and  $x/L = 0.7$  in Fig. 6. This graph displays the corresponding velocity distribution of Fig. 5 contours. At the first stage of microchannel,  $x/L = 0.3$ , velocity profile is entirely symmetric and almost fully developed. The second location of plots,  $x/L = 0.7$ , is after ONB point on the microchannel bottom surface, and its velocity profile is asymmetrical. Small bubbles that are stuck to the bottom surface of the channel ( $y/h_{ch} = 0$ ) are blocking liquid passage partially. This blockage has caused an asymmetry in velocity profile. In the last location of plots,  $x/L = 0.96$ , velocity of the detaching bubble is also included in velocity distribution. It can be observed that in the two-phase region each phase has different velocity magnitude, and therefore, models with the assumption of equal velocity distribution in both phases cannot capture these velocity differences.

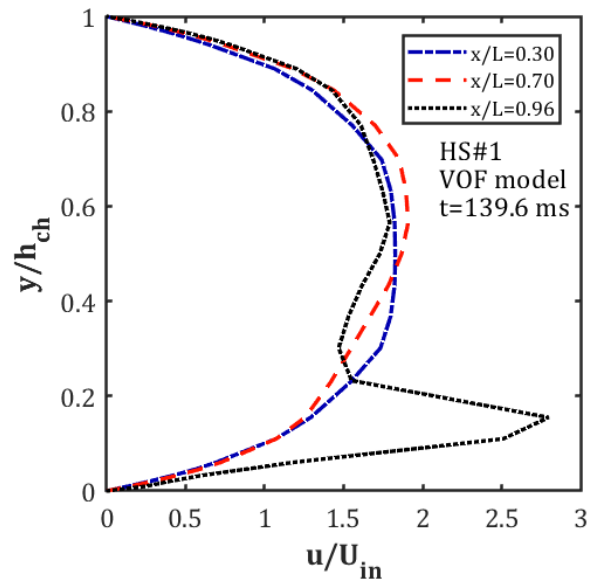


Figure 6. non-dimensional velocity distribution of VOF model at three sections of HS#1 at 139.6 ms.

#### 4. Conclusion

In this research, subcooled flow boiling in two microchannel heat sinks is studied numerically. In order to compare different numerical approaches to simulate this phenomenon, results of five numerical models, including volume of fluid (VOF) model, EulBoil model, EulLee model, EulTPC model, and mixture model were presented. The average bottom wall temperature at steady-state condition was predicted with less than 2% error with respect to experimental value by VOF and EulTPC models. At this working condition, nucleate boiling regime was expected, and only VOF model predicted this regime properly. Flow and thermal specifications of a detaching bubble from microchannel bottom surface were studied. It was observed that after start of nucleate boiling, velocity profile is not symmetric anymore. It was

concluded that models with assumption of equal velocity distribution in both phases are incapable of capturing some flow specifications. As the main result of this research, the VOF model was introduced as the best model to simulate flow boiling and

predict wall temperature with high precision at the working conditions of this study. Subcooled flow boiling's capability to be used in thermal management systems was proved while observing temperature distribution over computational domain.

### Nomenclature

$c_p$	Heat capacity at constant pressure	$T$	Temperature
$CFL$	Courant number	$t$	Time
$D_w$	Bubble departure diameter	$t_{ch}$	Microchannel wall thickness
$E$	Energy	$T_w$	Average bottom wall temperature
$F$	External body force	$u$	Velocity in x direction
$F_{vm}$	Virtual mass force	$\vec{v}$	Velocity vector
$FPV$	Outgoing fluxes per volume of each cell	$w_{ch}$	Microchannel width
$G$	Mass flux	<i>Greek symbols</i>	
$g$	Gravity	$\alpha$	Volume fraction
$h$	Enthalpy	$\mu$	Dynamic viscosity
$h_{ch}$	Microchannel height	$\rho$	Density
$h_{hs}$	Heat sink height	<i>Subscripts</i>	
$k$	Thermal conductivity	$in$	Inlet
$L$	Microchannel length	$l$	Liquid
$\dot{m}_{lv}$	Evaporation mass transfer	$q$	Related to qth phase
$p$	Pressure	$sat$	Saturation
$Q$	Intensity of heat exchange	$sub$	Subcooled
$q''$	Heat flux	$v$	Vapor
$R$	Interphase force	$w$	Wall
$S_h$	Volumetric heat source	$ch$	Channel

### 5. References

- [1] D. B. Tuckerman and R. F. W. Pease, "High-performance heat sinking for VLSI," *IEEE Electron Device Lett.*, vol. 2, no. 5, pp. 126–129, May 1981.
- [2] C. L. Ong and J. R. Thome, "Macro-to-microchannel transition in two-phase flow: Part 1 – Two-phase flow patterns and film thickness measurements," *Exp. Therm. Fluid Sci.*, vol. 35, no. 1, pp. 37–47, Jan. 2011.
- [3] G. Karniadakis, A. Beskok, and N. Aluru, *Microflows and Nanoflows*, vol. 29. New York: Springer-Verlag, 2005.
- [4] M. Hatami and D. D. Ganji, "Thermal and flow analysis of microchannel heat sink (MCHS) cooled by Cu–water nanofluid using porous media approach and least square method," *Energy Convers. Manag.*, vol. 78, pp. 347–358, Feb. 2014.
- [5] B. H. Salman, H. A. Mohammed, K. M. Munisamy, and A. S. Kherbeet, "Characteristics of heat transfer and fluid flow in microtube and microchannel using conventional fluids and nanofluids: A review," *Renew. Sustain. Energy Rev.*, vol. 28, pp. 848–880, Dec. 2013.
- [6] A. K. M. M. Morshed, F. Yang, M. Yakut Ali, J. A. Khan, and C. Li, "Enhanced flow boiling in a microchannel with integration of nanowires," *Appl. Therm. Eng.*, vol. 32, no. 1, pp. 68–75, Jan. 2012.
- [7] T. Harirchian and S. V. Garimella, "Flow regime-based modeling of heat transfer and pressure drop in microchannel flow boiling," *Int. J. Heat Mass Transf.*, vol. 55, no. 4, pp. 1246–1260, Jan. 2012.
- [8] B. Agostini, J. R. Thome, M. Fabbri, B. Michel, D. Calmi, and U. Klöter, "High heat flux flow boiling in silicon multi-microchannels – Part I: Heat transfer characteristics of refrigerant R236fa," *Int. J. Heat Mass Transf.*, vol. 51, no. 21–22, pp. 5400–5414, Oct. 2008.
- [9] P. C. Lee and C. Pan, "Boiling heat transfer and two-phase flow of water in a single shallow microchannel with a uniform or diverging cross section," *J. Micromechanics Microengineering*, vol. 18, no. 2, p. 025005, Feb. 2008.
- [10] J. Lee and I. Mudawar, "Fluid flow and heat transfer characteristics of low temperature two-phase micro-channel heat sinks – Part 1: Experimental methods and flow visualization results," *Int. J. Heat Mass Transf.*, vol. 51, no.

- 17–18, pp. 4315–4326, Aug. 2008.
- [11] G. Oguntala, R. Abd-alhameed, G. Sobamowo, and I. Danjuma, “Performance, thermal stability and optimum design analyses of rectangular fin with temperature-dependent, thermal properties and Internal heat generation,” vol. 49, no. 1, pp. 37–43, 2018.
- [12] A. Alizadehdakhel, M. Rahimi, and A. A. Alsairafi, “CFD modeling of flow and heat transfer in a thermosyphon,” *Int. Commun. Heat Mass Transf.*, vol. 37, no. 3, pp. 312–318, Mar. 2010.
- [13] Y. W. Kuang, W. Wang, R. Zhuan, and C. C. Yi, “Simulation of boiling flow in evaporator of separate type heat pipe with low heat flux,” *Ann. Nucl. Energy*, vol. 75, pp. 158–167, Jan. 2015.
- [14] E. Abedini, A. Behzadmehr, S. M. H. Sarvari, and S. H. Mansouri, “Numerical investigation of subcooled flow boiling of a nanofluid,” *Int. J. Therm. Sci.*, vol. 64, pp. 232–239, Feb. 2013.
- [15] I. Behroyan, P. Ganesan, S. He, and S. Sivasankaran, “CFD models comparative study on nanofluids subcooled flow boiling in a vertical pipe,” *Numer. Heat Transf. Part A Appl.*, vol. 73, no. 1, pp. 55–74, Jan. 2018.
- [16] A. Mukherjee and S. G. Kandlikar, “Numerical simulation of growth of a vapor bubble during flow boiling of water in a microchannel,” *Microfluid. Nanofluidics*, vol. 1, no. 2, pp. 137–145, May 2005.
- [17] A. Mukherjee, S. G. Kandlikar, and Z. J. Edel, “Numerical study of bubble growth and wall heat transfer during flow boiling in a microchannel,” *Int. J. Heat Mass Transf.*, vol. 54, no. 15–16, pp. 3702–3718, Jul. 2011.
- [18] M. Magnini, B. Pulvirenti, and J. R. Thome, “Numerical investigation of hydrodynamics and heat transfer of elongated bubbles during flow boiling in a microchannel,” *Int. J. Heat Mass Transf.*, vol. 59, no. 1, pp. 451–471, Apr. 2013.
- [19] C. Fang, M. David, A. Rogacs, and K. Goodson, “VOLUME OF FLUID SIMULATION OF BOILING TWO-PHASE FLOW IN A VAPOR-VENTING MICROCHANNEL,” *Front. Heat Mass Transf.*, vol. 1, no. 1, Jun. 2010.
- [20] R. Zhuan and W. Wang, “Flow pattern of boiling in micro-channel by numerical simulation,” *Int. J. Heat Mass Transf.*, vol. 55, no. 5–6, pp. 1741–1753, Dec. 2011.
- [21] R. Zhuan and W. Wang, “Simulation of subcooled flow boiling in a micro-channel,” *Int. J. Refrig.*, vol. 34, no. 3, pp. 781–795, May 2011.
- [22] ANSYS FLUENT, “User’s Guide (Release 18.2).” ANSYS Inc, 2017.
- [23] W. H. Lee, “A pressure iteration scheme for two-phase modeling,” *Los Alamos Sci. Lab. Los Alamos, New Mex. Tech. Rep. LA-UR*, pp. 79–975, 1979.
- [24] N. Kurul, “On the modeling of multidimensional effects in boiling channels,” *ANS. Proc. Natl. Heat Transf. Con.* Minneapolis, Minnesota, USA, 1991, 1991.
- [25] V. I. Tolubinsky and D. M. Kostanchuk, “Vapour bubbles growth rate and heat transfer intensity at subcooled water boiling,” in *International Heat Transfer Conference 4*, 1970, vol. 23.
- [26] M. Misale, G. Guglielmini, and A. Priarone, “HFE-7100 pool boiling heat transfer and critical heat flux in inclined narrow spaces,” *Int. J. Refrig.*, vol. 32, no. 2, pp. 235–245, Mar. 2009.